

Self-interacting freeze-in dark matter in a singlet doublet scenario

Purusottam Ghosh,^a Partha Konar,^b Abhijit Kumar Saha,^c and Sudipta Show^{b,d}

^aRegional Centre for Accelerator-based Particle Physics, Harish-Chandra Research Institute, HBNI, Chhatnag Road, Jhansi, Allahabad - 211 019, India

^bTheoretical Physics Division, Physical Research Laboratory, Shree Pannalal Patel Marg, Ahmedabad - 380009, Gujarat, India

^cSchool of Physical Sciences, Indian Association for the Cultivation of Science, 2A & 2B Raja S.C. Mullick Road, Kolkata 700 032, India

^dIndian Institute of Technology, Gandhinagar - 382424, Gujarat, India

E-mail: purusottamghosh@hri.res.in, konar@prl.res.in, psaks2484@iacs.res.in, sudipta@prl.res.in

Abstract. We examine the non-thermal production of dark matter in a scalar extended singlet doublet fermion model where the lightest admixture of the fermions constitutes a suitable dark matter candidate. The dark sector is non-minimal with the MeV scale singlet scalar, which is stable in the Universe lifetime and can mediate the self-interaction for the multi-GeV fermion dark matter mitigating the small scale structure anomalies of the Universe. If the dark sector is strongly coupled, it undergoes internal dark thermal equilibrium after freeze-in production, and we end up with suppressed relic abundance for the fermion dark matter in a radiation dominated Universe. In contrast, the presence of a modified cosmological phase in the early era drives the fermion dark matter to satisfy nearly the whole amount of observed relic. It also turns out that the assumption of an unconventional cosmological history can allow the GeV scale dark matter to be probed at LHC from displaced vertex signature with improved sensitivity.

Keywords: Dark matter, Freeze in, Self-interacting, Collider search

Contents

1	Introduction	1
2	The Model	3
3	Dark matter relic	4
3.1	Radiation dominated Universe	4
3.2	Non-standard Universe	7
3.2.1	Faster than kination phase	8
3.2.2	Kination phase	10
4	Discussion on Collider searches	13
5	Dark matter self-interaction	15
6	Summary and Conclusion	17
A	Cross section	18
B	Decay widths	18
C	Energy Transfer rate from SM to dark sector	19

1 Introduction

In the sea of apparent voidness at experimental fronts, some remarkable signs of progress have recently been made in dark matter theory, with new elegant ideas concerning dark matter production mechanisms and the nature of its interaction. One of the exciting proposals is the non-thermal origin of dark matter production known as an *freeze-in* [1]. The freeze-in process holds under the assumption that the dark matter is feebly coupled to the visible sector and initially having zero number density. At a later stage, it can be produced non-thermally from decay or scattering of visible sector particles.

On another front, the collisionless cold dark matter paradigm suffers from small scale structure anomalies such as *cusp vs core* [2–4] and the *too-big-to-fail* problems [4–6] *etc.* As a resolution it has been proposed that the self-interaction [7–12], a form of non-gravitational interactions of Dark Matter (DM), is capable of addressing the problems associated with the small scale structure. Tight constraints on dark matter self-interactions come in terms of the ratio of such self-scattering cross section over DM mass from observations at Bullet Cluster and N-body simulations [4, 13].

Studies related to self-interacting dark matter in a typical WIMP (weakly interacting massive particle) paradigm are prevalent in literature (see, for example, [14–18] for some of the recent works). On the other hand, proposals for self-interacting dark matter with freeze-in production are somewhat limited and can be found in refs. [19, 20]. In ref. [20], the dark matter is fermionic in nature, and it self-interacts via a light scalar mediator. Similar analysis has been exercised in ref. [19], considering a vector dark matter candidate.

Irrespective of the production mechanisms, a strong dark matter self-interaction craves for a light mediator with mass ranging from keV to MeV scale. Another notable aspect is the dark sector thermalisation [20] due to the strong interaction between the dark matter and the light mediator. This reduces the relic abundance of DM after its freeze-in production. To avoid that, restriction on the mediator mass turns severe and lowers it towards $\mathcal{O}(1)$ KeV.

In this paper, we attempt to offer a freeze-in production [1] scenario of GeV scale vector fermion DM that carries a bright prospect of testability at collider experiments and is capable of alleviating small scale structure problems by undergoing sufficient self-interaction. In view of this, we adopt the singlet doublet framework where the dark matter (χ) turns out to be the lightest admixture of the singlet and doublet [21–48]¹. We extend the set-up by adding one gauge singlet real scalar (ϕ) field. The new scalar mediates the self-interaction for the fermion dark matter candidate. Additionally, it has no decay mode and is hence stable in Universe lifetime. The singlet doublet dark matter model has rich collider signatures as explored in [26, 49, 50]. The heavier charged fermion or neutral partner is part of the additional $SU(2)_L$ doublet fermion. Their copious production at colliders is expected due to the $SU(2)_L$ gauge mediated interactions. The long-lived charged particle could give rise to disappearing charge tracks, whereas the long-lived heavier neutral particle can be traced through searching displaced vertices at LHC.

We focus on working in a scenario where the GeV scale fermion dark matter predominantly contribute to the total relic abundance. Stronger interaction strength between the fermionic dark matter and the mediator scalar is desired for producing large self-interaction [14, 15, 19, 20, 51]. On the other hand, a strongly coupled dark sector generally leads to the formation of internal dark thermal equilibrium with a separate dark sector temperature T_D [20, 52–56]. In our present scenario, after the freeze-in production of χ , they start annihilating into a pair of ϕ and vice versa, maintaining the dark sector equilibrium before a freeze-out mechanism triggers for χ . In literature, such rich dynamics inside a hidden dark sector is familiarly known as the reannihilation effect. Considering radiation dominated Universe (RD), we find that after the dark sector freezes out, ϕ shares a sizeable contribution to the total relic abundance. Thus, a χ dominated scenario is very unlikely.

Since our aim is to provide a χ dominated scenario which may also give rise to velocity-dependent fermionic self-interacting dark matter (see [20] for a similar exercise in a different framework), the proposed set up as discussed above in the radiation dominated Universe does not work. In the present study, we apprehend that the presence of a non-standard epoch in the early Universe could be useful to alleviate this. A faster expansion of the Universe can prevent the dark sector from reaching thermal equilibrium or slow down the dark sector interaction rate. These assist in suppressing the $\chi\chi \rightarrow \phi\phi$ conversion rate to obtain a χ dominated dark matter scenario. We have employed two particular kinds of modified cosmology [45, 47, 57] namely kination domination and faster than kination domination. We have found that such non-standard epochs in the early Universe can work remarkably to reach our defined aim of obtaining $\Omega_\chi h^2 \sim 0.12$ [58] which has the potential to resolve the cosmological problems as earlier stated. Additionally, the presence of a non-standard epoch helps to provide a complementary probe of the GeV scale dark matter in the singlet doublet framework via displaced vertices which is not possible in a radiation dominated scenario as shown in [49, 50].

¹Earlier works [49, 50] on singlet doublet freeze-in dark matter reveal that the dark matter is mostly singlet dominated with vanishing mixing angle with the doublet.

The paper is organised as follows. In section 2, we furnish the model structure and the corresponding Lagrangians. Next, in section 3, we discuss the dark matter phenomenology considering the standard cosmology and two different forms of non-standard cosmology. We describe the discovery prospects of the proposed model at collider experiments in section 4. Estimate of the self-interaction cross section for the singlet doublet dark matter are presented in section 5. Finally, we summarise by pointing out the new findings of our analysis and draw the conclusion in section 6.

2 The Model

We extend the SM particle content by one $SU(2)_L$ doublet fermion (Ψ) with hypercharge $Y = -\frac{1}{2}$ and one hyperchargeless gauge singlet vector fermion (χ). In addition, we also include a real scalar singlet field (ϕ) which assists the DM to yield strong dark matter self-interaction. We impose a discrete Z_2 symmetry under which the SM particles and the ϕ field transform trivially while the BSM fermions are assigned odd Z_2 charges. The Lagrangian of the scalar sector is read as

$$\mathcal{L}_{\text{scalar}} = |D^\mu H|^2 + \frac{1}{2}(\partial^\mu \phi)(\partial_\mu \phi) - V(H, \phi), \quad (2.1)$$

where the covariant derivative is defined as,

$$D^\mu = \partial^\mu - ig \frac{\sigma^a}{2} W^{a\mu} - ig' \frac{Y}{2} B^\mu, \quad (2.2)$$

with g and g' being the $SU(2)_L$ and the $U(1)_Y$ gauge couplings respectively. The scalar potential $V = V(H) + V(\phi) + V(\phi, H)$ takes the following form,

$$V(H) = -\mu_H^2 (H^\dagger H) + \lambda_H (H^\dagger H)^2, \quad (2.3)$$

$$V(\phi) = \frac{m_\phi^2}{2} \phi^2 + \frac{\lambda_\phi}{4!} \phi^4 + \frac{b_3}{3!} \phi^3, \quad (2.4)$$

$$V(\phi, H) = \frac{\lambda_{\phi H}}{2} \phi^2 (H^\dagger H) + a_3 \phi (H^\dagger H). \quad (2.5)$$

Note that we do not write the linear term for ϕ in $V(\phi)$ since it can always be absorbed through the redefinition of the other parameters. We assume that all the mass scales and the coupling coefficients are real and positive. In this limit, the vacuum expectation values (vev) of the scalars H and ϕ after minimising the potential V are obtained as,

$$\langle H \rangle = v, \quad \langle \phi \rangle = 0. \quad (2.6)$$

The Lagrangian for the fermionic sector is written as,

$$\mathcal{L} = \mathcal{L}_f + \mathcal{L}_Y, \quad (2.7)$$

where,

$$\mathcal{L}_f = i\bar{\Psi}\gamma_\mu D^\mu \Psi + i\bar{\chi}\gamma_\mu \partial^\mu \chi - m_\Psi \bar{\Psi}\Psi - m_\chi \bar{\chi}\chi \quad (2.8)$$

$$\mathcal{L}_Y = -Y\bar{\Psi}\tilde{H}\chi + h.c. - \lambda\phi\bar{\chi}\chi - \delta\phi\bar{\Psi}\Psi, \quad (2.9)$$

where we have defined $\Psi^T = (\psi^+ \ \psi^0)$.

The Dirac mass matrix for the neutral fermions after the spontaneous breakdown of the electroweak symmetry is obtained as,

$$\mathcal{M}_D = \begin{pmatrix} m_\Psi & M_D \\ M_D & m_\chi \end{pmatrix}, \quad (2.10)$$

where we define $M_D = \frac{Yv}{\sqrt{2}}$. After diagonalisation of Eq.(2.10), we are left with two neutral Dirac particles which we identify as ξ_1 and ξ_2 . The mass eigenvalues of ξ_1 and ξ_2 are given by,

$$m_{\xi_1} \approx m_\chi - \frac{M_D^2}{m_\Psi - m_\chi} \quad (2.11)$$

$$m_{\xi_2} \approx m_\Psi + \frac{M_D^2}{m_\Psi - m_\chi} \quad (2.12)$$

Therefore, the lightest eigenstate is ξ_1 , which is the stable DM candidate of our framework. The stability of the DM is ensured by the unbroken \mathcal{Z}_2 symmetry. The mixing between two flavor states, *i.e.* neutral part of the doublet (ψ^0) and the singlet field (χ) is parameterised by,

$$\sin 2\theta \simeq \frac{2Yv}{\Delta M}, \quad (2.13)$$

where $\Delta M = m_{\xi_2} - m_{\xi_1} \approx m_\Psi - m_\chi$ in the small Y limit. Here, ξ_1 can be identified with the singlet χ . Since the present analysis involves freeze-in dark matter production, the mixing between the singlet and doublet fermions is always very tiny. Therefore, henceforward we identify the dark matter candidate as χ .

3 Dark matter relic

The present set-up has two stable particles ϕ and χ , and both can contribute to total DM relic abundance. The relative contribution of each component to the DM relic is dependent on early Universe history, as we discuss below. We have worked with $m_\phi \ll m_\chi$ and $\lambda \sim \mathcal{O}(10^{-1})$ with an aim to obtain a large amount of self-interaction for χ that can address the problems associated with small scale structures of the Universe. Irrespective of the cosmological history of the Universe, we assume $a_3, \lambda_{\phi H}, \delta, Y \ll 1$ always such that both ϕ and χ can never equilibrate with the SM bath. Additionally, we have considered a specific choice $a_3, \delta, \lambda_{\phi H} \ll Y$ which implies ϕ can only be populated at a non-negligible rate (depending on the expansion rate of the Universe) from the $\chi\chi \rightarrow \phi\phi$ process.

3.1 Radiation dominated Universe

In the standard description of Big bang cosmology, the Universe is radiation dominated prior to BBN. Initially both the components begin with zero number density and first χ gets produced from the SM bath. To be specific, production of χ at early Universe occurs primarily from Ψ decay with thermally averaged decay width $\langle \Gamma_\Psi \rangle^T$ where T is the SM temperature. Before EW symmetry breaking, the DM production takes place only from the $Y\Psi\tilde{H}\chi$ vertex. After EW symmetry breaking, the production channels for DM are namely, $\psi^\pm \rightarrow \chi W^\pm$, $\xi_2 \rightarrow \chi Z$ and $\xi_2 \rightarrow \chi h$. In order to express the χ production rate as function of temperature, we define $\langle \Gamma_\Psi \rangle^T = \langle \Gamma_\Psi \rangle \Theta(T - T_{\text{EW}}) + \langle \Gamma_{\Psi^\pm} + \Gamma_{\xi_2} \rangle \Theta(T_{\text{EW}} - T)$ where $T_{\text{EW}} \sim 160$

	λ	m_Ψ	m_χ	m_ϕ	Y	$\Omega_\chi h^2$	$\Omega_\phi h^2$
RD-I	0.13	1.5 TeV	20 GeV	10 MeV	5.40×10^{-10}	0.01	0.11
RD-II	0.085	1.5 TeV	10 GeV	10 MeV	5.45×10^{-10}	0.01	0.11

Table 1. Two representative benchmark points that describe the reannihilation scenario in the present framework considering radiation dominated Universe.

GeV indicates the EW symmetry breaking temperature. Subsequently, the $\chi\chi \rightarrow \phi\phi$ process yields ϕ and when the number density of ϕ is sufficient, it can further annihilate to χ and form a local dark sector thermal equilibrium with an uniform temperature T_D provided

$$r \equiv \frac{n_\chi \langle \sigma v \rangle_{\chi\chi \rightarrow \phi\phi}}{\mathcal{H}} \gg 1. \quad (3.1)$$

Finally χ freezes out and both contribute non-negligibly to the total relic abundance. The set of Boltzman equations that governs such dynamics with $z (= \frac{m_\chi}{T})$ are given by [20, 52–56],

$$\frac{dY_\phi}{dz} = \frac{s}{\mathcal{H}z} \langle \sigma v \rangle_{\chi\chi \rightarrow \phi\phi}^{T_D} \left[Y_\chi^2 - \left(\frac{Y_\chi^{\text{eq}}(T_D)}{Y_\phi^{\text{eq}}(T_D)} \right)^2 Y_\phi^2 \right] \quad (3.2)$$

$$\frac{dY_\chi}{dz} = -\frac{s}{\mathcal{H}z} \langle \sigma v \rangle_{\chi\chi \rightarrow \phi\phi}^{T_D} \left[Y_\chi^2 - \left(\frac{Y_\chi^{\text{eq}}(T_D)}{Y_\phi^{\text{eq}}(T_D)} \right)^2 Y_\phi^2 \right] + \frac{45z^2}{2\pi^2 m_\chi^3} \frac{s \langle \Gamma_\Psi \rangle^T}{\mathcal{H}} (Y_\Psi^{\text{eq}}(T) - Y_\chi). \quad (3.3)$$

To evaluate the dark temperature (T_D) one needs to solve the Boltzman equation for the total dark sector energy density ($\rho_D = \rho_\chi + \rho_\phi$) where ρ_i indicates the energy density for an individual component [20, 51–53, 56, 59, 60].

$$\frac{d\rho_D}{dt} + 3H(\rho_D + p_D) = \mathcal{P}_\Psi n_\Psi^{\text{eq}}, \quad (3.4)$$

where the quantity \mathcal{P}_Ψ represents the thermally averaged energy transfer rate from the SM to dark sector. The notation $p_D = p_\chi + p_\phi$ stands for the sum of the pressures for individual components. The standard form of p_D is given by,

$$p_D = \frac{g_\chi}{6\pi^2} \int_{m_\chi}^{\infty} \frac{(E_\chi^2 - m_\chi^2)^{3/2}}{e^{E_\chi/T_D} + 1} dE_\chi + \frac{g_\phi}{6\pi^2} \int_{m_\phi}^{\infty} \frac{(E_\phi^2 - m_\phi^2)^{3/2}}{e^{E_\phi/T_D} + 1} dE_\phi, \quad (3.5)$$

The symbols g_χ and g_ϕ imply the internal degrees of freedom for χ and ϕ species. Additionally, one can write the energy density of the dark sector as,

$$\rho_D = \frac{g_\chi}{2\pi^2} \int \frac{(E_\chi^2 - m_\chi^2)^{1/2} E_\chi^2 dE_\chi}{e^{\frac{E_\chi}{T_D}} + 1} + \frac{g_\phi}{2\pi^2} \int \frac{(E_\phi^2 - m_\phi^2)^{1/2} E_\phi^2 dE_\phi}{e^{\frac{E_\phi}{T_D}} + 1}. \quad (3.6)$$

Analytical computation of the integrations in RHS of Eqs.(3.5-3.6) in presence of Fermi-Dirac distribution function looks complicated. Instead one can compute the same in the Maxwell

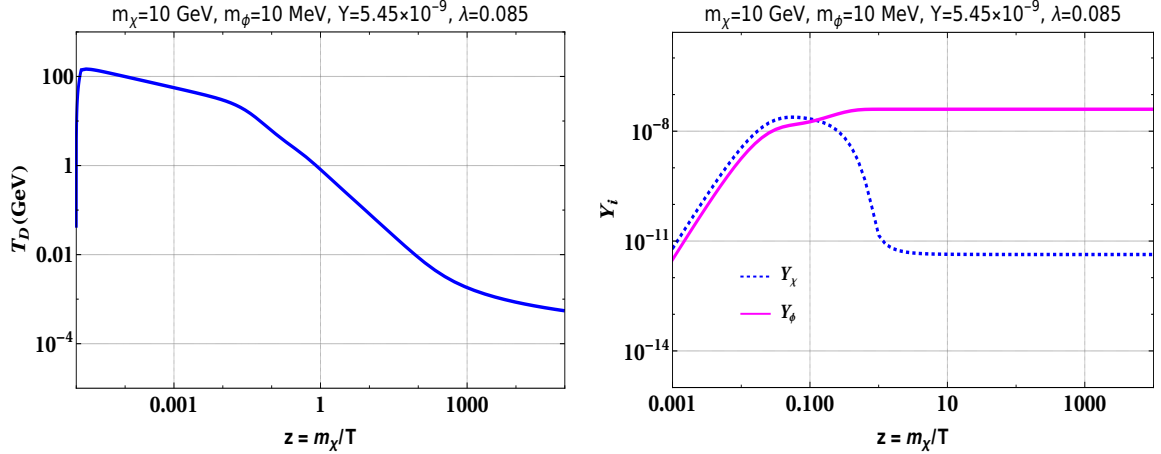


Figure 1. The left plot shows the variation of dark sector temperature T_D as a function of inverse temperature z . Corresponding evolutions for the number densities of dark sector particles are shown in the right plot. Here, after initial non-thermal production of χ strong self-interaction generates a dark sector thermal equilibrium. Further, freeze-out produces the ϕ abundance. The figures are computed considering the benchmark point RD-II in Table 1.

Boltzman-approximation. We find ²,

$$p_D = \frac{g_\chi}{2\pi^2} m_\chi^2 T_D^2 K_2 \left(\frac{m_\chi}{T_D} \right) + \frac{g_\phi}{2\pi^2} m_\phi^2 T_D^2 K_2 \left(\frac{m_\phi}{T_D} \right) \quad (3.7)$$

$$\rho_D = \frac{g_\chi m_\chi^2}{2\pi^2} T_D \left[m_\chi K_1 \left(\frac{m_\chi}{T_D} \right) + 3T_D K_2 \left(\frac{m_\chi}{T_D} \right) \right] + \frac{g_\phi m_\phi^2}{2\pi^2} T_D \left[m_\phi K_1 \left(\frac{m_\phi}{T_D} \right) + 3T_D K_2 \left(\frac{m_\phi}{T_D} \right) \right]. \quad (3.8)$$

Replacing Eq.(3.7) and Eq.(3.8) in Eq.(3.4), it is simple obtain the evolution equation for T_D as function of SM temperature.

In Table 1, we provide two reference points that instigate dark freeze out of χ after the non-thermal production from the SM bath for two choices of dark matter masses having magnitude 10 GeV and 20 GeV, respectively. The evolutions of dark sector temperature and χ and ϕ abundances for the benchmark point RD-II (with DM mass 10 GeV) are shown in Figure 1. To generate these figures, we solve the set of coupled Boltzmann equations as described in Eqs.(3.3-3.6) and also used Eqs.(3.7-3.8) with the initial conditions $(Y_\chi, Y_\phi, T_D) = 0$ and $Y_\Psi = Y_\Psi^{\text{eq}}(T)$. In Figure 2, we display the ratio r as defined in Eq.(3.1) to measure the strength of dark sector interaction rate as a function of SM temperature for the same benchmark point. This figure confirms the formation of dark sector equilibrium after the non-thermal production of both the components with $r \gg 1$ for a finite period. In the left of Figure 1, we see the evolution pattern of the dark temperature as a function of SM bath temperature. Since the dark matter annihilation to SM particles is negligible, it turns out that $T_D \ll T$ always. Initially, the dark temperature increases from zero due to constant entropy injection from the SM bath and reaches a maximum value. Then, due to the expansion of the Universe, it keeps decreasing. Till $T \sim m_\Psi$, the production of χ

²We verified a close match between the numerical estimation from the standard expression with this approximation for our calculation.

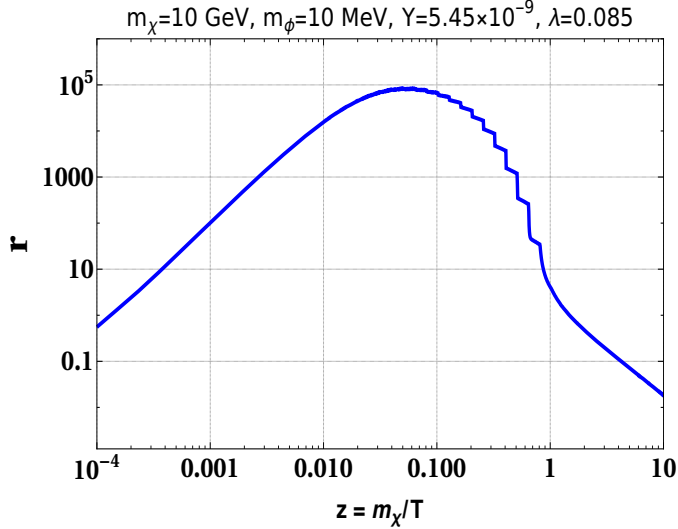


Figure 2. The ratio of the interaction rate among the dark sector particles and Hubble parameter of the Universe following Eq.(3.1) as function of temperature for for the benchmark point RD-II in Table 1.

continues from Ψ decay, and hence we see a slower decreasing rate of T_D initially, and after that, it becomes steep.

The most intriguing part is, here, due to large λ , the χ keeps annihilating to ϕ till the decoupling and ends with suppressed abundance (see right of Figure 1). Hence for the chosen benchmark points in the reannihilating scenario, we notice $\Omega_\chi \ll \Omega_\phi$. An enhancement of λ for a fixed m_χ may slightly increase the relic of ϕ further, while it will be reduced further in the opposite limit. However, a small λ is not desirable in view of generating sufficient self-interaction of χ to solve the small scale structure problems of the Universe. It is to note that for both the reference points in Table 1, the total relic abundance $\Omega_T h^2 = \Omega_\phi h^2 + \Omega_\chi h^2 \sim 0.12$ [58] remains within the observed limit by Planck requiring a similar order of Y value.

Thus, radiation dominated Universe with a large λ fails to provide a pure χ dominated scenario due to the late time annihilation of the dark matter χ to mediator ϕ . We anticipate that a non-standard Universe in the form of kination or faster than kination domination could enforce significant suppression of ϕ production rate from $\chi\chi \rightarrow \phi\phi$ process even in the presence of large λ . This may occur if the ratio in Eq.(3.1) remains comparatively suppressed till late time. Note that such faster expansion of the Universe may also slow down the production rate of χ from the SM bath. However, that can be increased by adjusting Y .

3.2 Non-standard Universe

In standard description of cosmology, we generally assume that the Universe is radiation dominated in the pre big bang nucleosynthesis (BBN) era. However, due to lack of evidences, possibilities remain open that before BBN, the Universe could have been occupied by a nonstandard fluid, redshifting faster or slower than the radiation component. Earlier works have emphasised that consideration of such modified cosmology poses non-trivial impact on the dark matter phenomenology.

A non-standard Universe can be sketched by assuming the presence of an additional species (η) along with the radiation component in the Universe. We consider the equation

	λ	m_Ψ	m_χ	m_ϕ	Y	n	T_r	$\Omega_\chi h^2$
FKD-I	0.13	1.5 TeV	20 GeV	10 MeV	2×10^{-8}	3	20 MeV	0.119
FKD-II	0.085	1.5 TeV	10 GeV	10 MeV	2.44×10^{-8}	3	22 MeV	0.119

Table 2. Two representative benchmark points that demonstrate *pure freeze-in* non-standard cosmology with faster than kination domination.

of parameter (ω) of the nonstandard fluid is larger than that of radiation. We parameterize this by $\rho_\eta \propto a^{-3(1+\omega)}$ which can be converted to $\rho_\eta \propto a^{-(4+n)}$ with $\omega = \frac{1}{3}(n+1)$ and $n > 0$. The modified description of the Universe leads to the redefinition of the Hubble parameter (\mathcal{H}) as given by [45, 47, 57],

$$\mathcal{H}^2 = \frac{\rho_R + \rho_\eta}{3M_P^2}, \quad (3.9)$$

where M_P refers the reduced Planck scale, ρ_R and ρ_η correspond to the energy densities of radiation and η component. The total energy density of the Universe in presence of η as function of temperature can be expressed as,

$$\rho(T) = \rho_{\text{rad}}(T) + \rho_\eta(T) \quad (3.10)$$

$$= \rho_{\text{rad}}(T) \left[1 + \frac{g_*(T_r)}{g_*(T)} \left(\frac{g_{*s}(T)}{g_{*s}(T_r)} \right)^{(4+n)/3} \left(\frac{T}{T_r} \right)^n \right], \quad (3.11)$$

where $\rho_R = \frac{\pi^2}{30} g_*(T) T^4$ with g_* stands for the number of relativistic degrees of freedom. The relativistic entropy degrees of freedom is denoted by g_{*s} . Thus a faster expanding Universe is simply parameterised by the set of (n, T_r) . A larger n or smaller T_r prompts the energy density of the Universe to redshift more faster. The temperature T_r implies the end of modified expansion rate and we get back the radiation dominated phase. In case of standard radiation dominated Universe, η field would be absent and we simply consider $\rho = \rho_{\text{rad}}$. The BBN observation on the number of relativistic degrees of freedom imposes a lower bound on T_r ($\gtrsim (15.4)^{1/n}$ MeV). A special case $n = 2$ (or $\omega = 1$) is familiar as kination domination phase. For $n > 2$, one has to consider scenarios faster than quintessence with negative potential. We refer the readers to [57], for a detailed description of a fast-expanding Universe. Below we separately discuss the cases for kination domination and faster than kination domination.

3.2.1 Faster than kination phase

As earlier mentioned a faster than kination phase is realised for $n > 2$. Here we consider $n = 3$. A faster expansion implies enhanced Hubble rate which can suppress the interaction rate among the dark sector particles. If the interaction rate among the dark sector particles gets heavily suppressed, that leads to the production of χ by pure freeze-in. In that case the governing Boltzman equation for χ looks very simple as given by [1, 61],

$$\frac{dY_\chi}{dz} = \frac{45z^2}{2\pi^2 m_\chi^3} \frac{s\langle\Gamma_\Psi\rangle^T}{\mathcal{H}} (Y_\Psi^{\text{eq}}(T) - Y_\chi). \quad (3.12)$$

Since the rate of the conversion process $\chi\chi \rightarrow \phi\phi$ is negligibly low in case of pure freeze-in, we do not estimate the relic of ϕ here, which is expected to be barely abundant in the present Universe. For the same reason, the computation of dark temperature is not essential here.

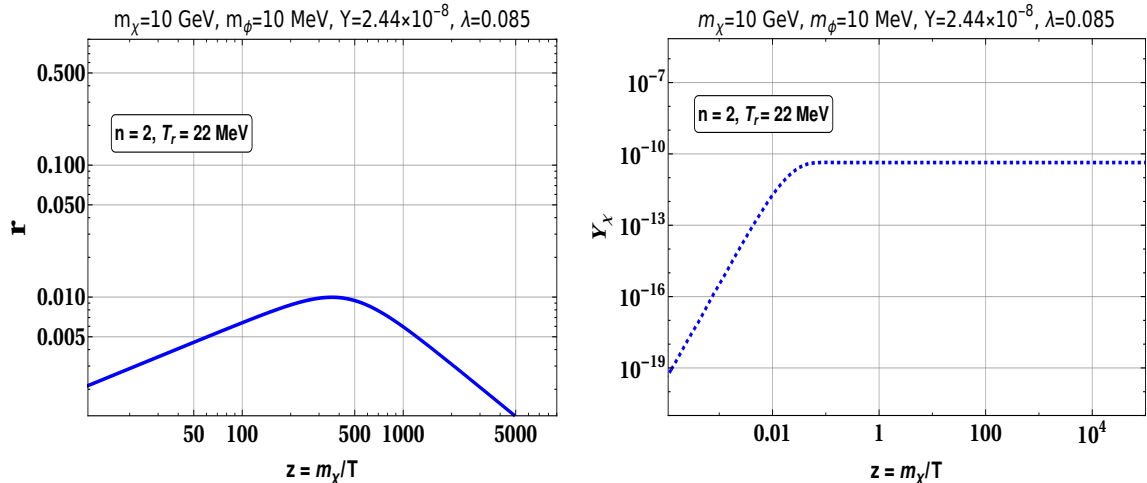


Figure 3. Left: The ratio of the interaction rate among the dark sector particles and Hubble parameter of the Universe as function of temperature for the benchmark point FKD-II in Table 2. Right: The evolution of DM comoving number density is shown with temperature for the same reference point.

In Table 2, we note down two benchmark points with BSM model inputs $\{\lambda, m_\Psi, m_\chi, m_\phi\}$ are same as used in section 3.1. We have considered zero initial abundance of χ since it remains out of equilibrium in the early Universe. We fix $n = 3$ for this case and vary the T_r and Y in order to obtain correct relic abundance (by pure freeze-in) as allowed by Planck. Recall that these two reference points have portrayed reannihilation patterns with $\Omega_\chi h^2 \ll \Omega_\phi h^2$ for a radiation dominated Universe. In the right of Figure 3, we have depicted the evolution of comoving abundance of χ with temperature considering the reference point FKD-II. We have used $n = 3$ and fixed the parameters T_r and Y such that correct relic abundance for χ is attained. In left of Figure 3, we estimate the parameter r as earlier defined and found it to be order of $\sim \mathcal{O}(10^{-2})$. This indeed ensures the validity of labelling the present scenario as *pure freeze-in*. Here we do not mention the abundance of the ϕ field. Owing to the faster expansion of the Universe, the produced χ never creates its own bath, and it is expected that the contribution of $\chi\chi \rightarrow \phi\phi$ would be negligible in yielding ϕ . Nevertheless, a conservative test can always be performed by solving the Boltzmann equations for Y_ϕ and Y_χ while considering the maximum³ possible value of $\langle\sigma v\rangle_{\chi\chi \rightarrow \phi\phi}$. By utilising this conservative method, we have found similar results (maximum uncertainty is 2%) with Y_ϕ remaining much lower than Y_χ . We also notice from Table 2, that the required order of the Yukawa coupling is relatively larger than the one shown in section 3.1 considering standard RD Universe. The reason is obvious as a faster expanding Universe not only suppresses the rate of $\chi\chi \rightarrow \phi\phi$ process but also slows down the production process of χ and therefore, one needs to raise BSM Yukawa coupling parameter Y appropriately. To investigate the T_r dependence on Y further, in Figure 4, we show the relic density satisfied contours in the $T_r - Y$ plane for $m_\chi = 10 \text{ GeV}$ and 20 GeV considering $n = 3$. We keep the corresponding values of λ and m_Ψ in accordance with Table 2. For a fixed DM mass, a smaller T_r requires larger Y . This occurs since a smaller T_r implies an enhanced Hubble rate, and it requires a larger Y to obey the relic abundance bound. Moreover, a smaller DM mass also requires larger Y to obey the

³Maximum possible value of a thermally averaged cross section can be found by equating the temperature of the corresponding bath with the heavier mass scale approximately associated with the interaction.

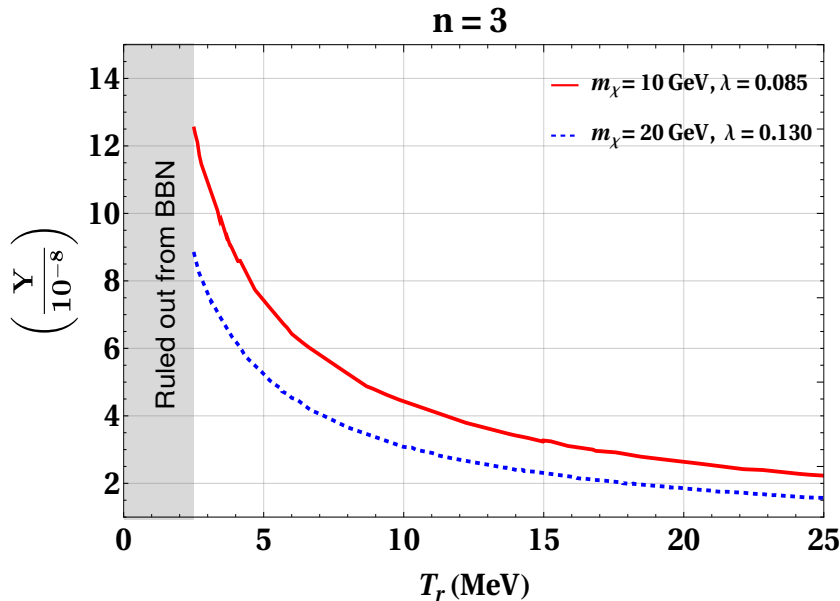


Figure 4. Relic satisfied contours in $T_r - Y$ plane considering $n = 3$ for $m_\chi = 10$ GeV and 20 GeV.

relic bound. It is to note that in Figure 4, we have kept T_r below 25 MeV. Beyond this value of T_r , the ratio r would turn larger than $\mathcal{O}(10)^{-2}$ and therefore, the contribution of $\chi\chi \rightarrow \phi\phi$ conversion in the final DM relic may turn important at some extent.

In summary, the above discussion reveals that a faster than kination dominated early Universe ($n = 3$) is able to provide a pure freeze-in yield for χ with absolutely dominant share to the total relic abundance even in the presence of $\lambda \sim \mathcal{O}(10^{-1})$. This is in sharp contrast to the RD Universe where we found $\Omega_\chi h^2 \ll \Omega_\phi h^2$ with the same values of λ and mass scales of the dark sector particles. In the upcoming section, we discuss how the scenario evolves in the case of kination dominated ($n = 2$) early Universe.

3.2.2 Kination phase

Earlier, we have seen, faster than kination domination has led to pure freeze-in for the parameters that show reannihilation in the case of an RD Universe by suppressing the interaction rate among dark sector particles. Now, we consider the kination domination case ($n = 2$), which leads to a relatively slower expansion rate of the Universe than $n = 3$ and hence may enhance the interaction rate inside the dark sector. Thus to realise pure freeze-in with kination domination era, a relatively smaller value of Y for a fixed T_r is expected to obey the relic bound compared to the $n = 3$ case. Indeed such prediction emerges to be correct as evident from Figure 5. Using the approximate method as commented earlier, we have found that for the respective ranges for Y and T_r in Figure 5, the ratio r always remains $\lesssim \mathcal{O}(10^{-2})$ and thus relic ϕ is always suppressed with an uncertainty 5% atmost.

One may also wonder whether a reannihilating scenario for the dark matter χ with final correct relic abundance is possible in non-standard cosmological models. To investigate this, let us stick to the $n = 2$ case. This would obviously require a larger T_r compared to the pure freeze-in case with $n = 2$. Assuming internal equilibrium of dark sector is established for some period in the early Universe, the set of Boltzman equations remain same as in

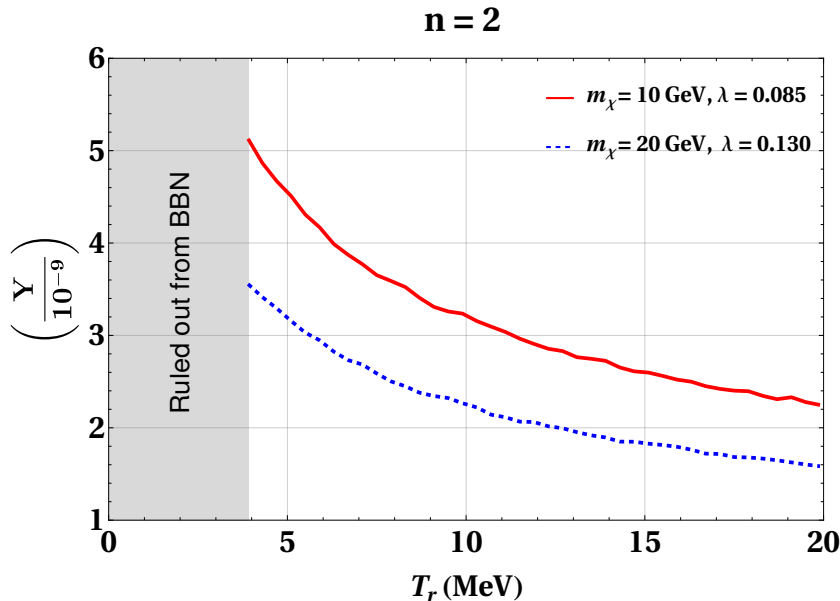


Figure 5. Relic satisfied contours in $T_r - Y$ plane for $m_\chi = 10$ GeV and 20 GeV considering $n = 2$.

	λ	m_Ψ	m_χ	m_ϕ	Y	n	T_r	$\Omega_\chi h^2$	$\Omega_\phi h^2$
KD-I	0.13	1.5 TeV	20 GeV	10 MeV	2.4×10^{-9}	2	320 MeV	0.115	0.003
KD-II	0.085	1.5 TeV	10 GeV	10 MeV	3.75×10^{-9}	2	180 MeV	0.118	0.001

Table 3. The representative benchmark points that lead to reannihilation after freeze-in production of χ in presence of kination dominated epoch with $n = 2$.

Eq.(3.2-3.4). We would like to reuse the same set of benchmark values for $(\lambda, m_\Psi, m_\chi, m_\phi)$ as originally introduced in section 3.1. We would like to emphasise that, these points depict a reannihilation pattern in the radiation dominated Universe, while the presence of a kination or faster than kination dominated epoch transform it to pure freeze-in with almost full χ occupancy in the total relic abundance provided suitable choices for T_r are made. Here, we find out the estimates of (Y, T_r) such that it shows a reannihilation pattern with $\Omega_\chi h^2 \gg \Omega_\phi h^2$. We consider zero initial abundance for the dark sector particles as well as $T_D^{\text{ini}} = 0$. In Table 3, we note down the required order of T_r and the Yukawa coupling that predicts such scenario considering the same set of $(\lambda, m_\Psi, m_\chi, m_\phi)$ as used in section 3.1.

The evolution patterns of Y_χ and Y_ϕ for the benchmark point KD-II in Table 3 are similar to the case of RD Universe as shown in Figure 6. In the left of Figure 6, the ratio r is plotted as a function of the temperature of the SM bath. This figure shows r crosses unity for a brief period and dark sector equilibrates. This feature enables χ to annihilate at a late time to ϕ after production from the standard model bath. However, the annihilation rate is suppressed due to faster expansion of the Universe, which results in reduced relic for ϕ as compared to the one in RD Universe. We also notice such an enhanced expansion rate of the Hubble parameter slows down the χ production process itself, but that can be adjusted by tuning the Yukawa coupling Y appropriately (see Table 3). In right of Figure 6, the temperature T_D is plotted as a function of SM temperature T . We see a nontrivial

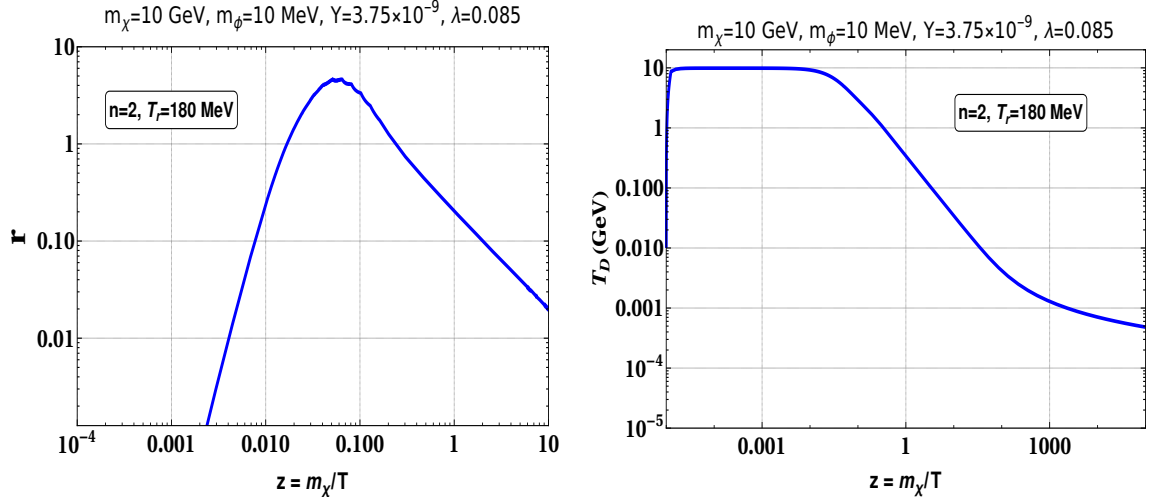


Figure 6. Left: The variation of parameter r is shown against the SM temperature for the reference point KD-II. Right: The variation of T_D on SM temperature T is shown for the same reference point.

pattern for the temperature evolution of the dark sector here. The T_D remains constant up to $z \sim 0.01$ then reduces with z . This has occurred specifically due to an accidental cancellation between the second term of LHS in Eq.(3.4) and the term in RHS while solving the Boltzman equation for dark sector energy density. Such cancellation is triggered by the same temperature dependence of the Hubble parameter and n_Ψ^{eq} when Ψ is relativistic. In Figure 7 the evolution patterns for the number densities of χ and ϕ considering the benchmark point KD-II are shown as function of SM temperature. The obtained patterns are similar as in case of RD Universe. The comoving number density of χ drops from its freeze-in value due to late time dark freeze out. A similar reannihilation pattern for $m_\chi = 20 \text{ GeV}$ can be obtained as well with the proper assignment of other relevant parameters as pointed out in Table 3. For both the benchmark points of Table 3, χ occupies the maximum share of total relic abundance, whereas ϕ can contribute up to 2% of the total relic.

Before we close this section, let us draw a clear comparison between the impacts of standard and non-standard cosmology within the present setup. We begin by fixing the mediator mass $m_\phi = 10 \text{ MeV}$ and dark matter at 10 GeV and 20 GeV , respectively. In an RD Universe, a larger value of λ (motivated from generating velocity dependent large self interaction) leads to the annihilation of χ to ϕ after its production by forming dark sector equilibrium. Consequently, we obtain ϕ as a dominant DM component rather than χ . We then anticipate that presence of a non-standard epoch (kination or faster than kination) in the early Universe can assist in realising a dominant share of χ in total DM relic abundance with or without reaching dark sector thermal equilibrium for the same dark sector parameters as used in the RD scenario. We have utilised the same benchmark points as used in the RD case and show that, indeed, a fast-expanding Universe changes the DM dynamics completely and helps in realising χ as the main dark matter component. This occurs since the presence of a modified cosmology enhance the expansion rate of the Universe and suppresses the conversion rate of the $\chi\chi \rightarrow \phi\phi$ process. One can also spot that it requires a larger amount of Yukawa coupling Y to obey the relic density bound in a non-standard era compared to the case in RD Universe. This, in turn, improves the collider search prospects of the present set up as we will talk about shortly.

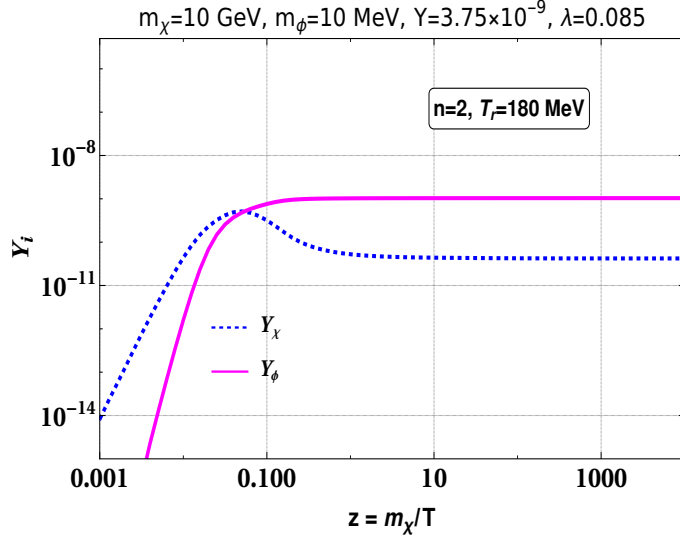


Figure 7. The evolution of χ and ϕ number densities are shown with SM temperature for the benchmark point KD-II.

4 Discussion on Collider searches

We shall now briefly discuss the detection prospects of the proposed singlet scalar extended singlet doublet fermion freeze-in DM at colliders. The possible collider signatures of the singlet doublet fermion DM model have been discussed in detail in the context of WIMP [41, 62] and FIMP [49, 50] DM scenarios. The collider sensitivity of the singlet doublet dark matter model is mainly based on the $Y\bar{\Psi}\tilde{H}\chi$ vertex. Note that the same vertex determines the production efficiency of the dark matter in the early Universe. Depending on the cosmological history and dark sector dynamics, we found that the value of Y keeps changing for fixed DM mass and m_Ψ or m_{ξ_2} . For example, a fast expanding Universe prefers larger Y as compared to the RD Universe in each of the pure freeze-in or reannihilation scenarios to obtain a constant dark matter relic. Therefore in the present framework, the colliders can perhaps be utilised to test the cosmological history at the early Universe and the hidden dark sector dynamics in the context of the singlet doublet model.

One of the possible signatures at LHC could be the disappearing charge track signature induced by $\psi^\pm \rightarrow \pi^\pm \xi_2$ decay with decay length $c\tau_{\psi^\pm} \sim \mathcal{O}(1)$ cm. Independent analyses by ATLAS and CMS collaborations [63, 64] have inferred strong restriction on the chargino mass considering a supersymmetric framework as a benchmark model. Since the decay $\psi^+ \rightarrow \pi^+ \xi_2$ is equivalent to chargino to Higgsino production, in the present analysis, the bounds provided by ATLAS and CMS can be employed in our analysis as well. In Figure 8, the purple shaded region is disfavored due to non-observation of disappearing charge track assuming $\text{Br}(\psi^\pm \rightarrow \pi \xi_2) \simeq 1$. In our analysis, we have considered m_Ψ to be of the TeV scale. Thus the bound arising from the disappearing charge track signature is not important for our case.

On the other hand, due to gauge mediated interactions, the heavy charged (ψ^\pm) and neutral (approximately ξ_2) components of dark fermion doublet in this model can be produced at a hadronic collider. The relevant processes are $pp \rightarrow \psi^+ \psi^-$, $\xi_2 \xi_2$ and $\psi^\pm \xi_2$ which further

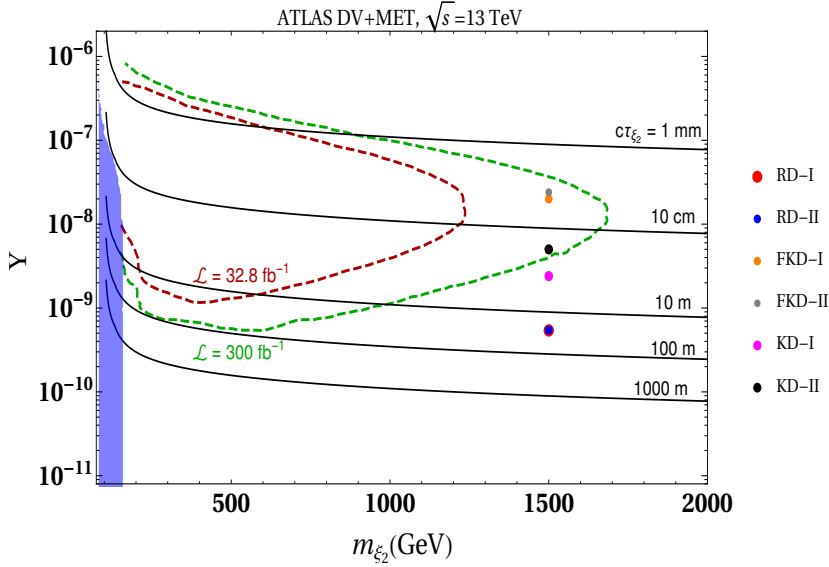


Figure 8. Discovery prospects of the chosen benchmark points (both in standard and non standard cosmology) in $Y - m_{\xi_2}$ plane. The blue region is disfavored by the search of disappearing charge track signature. We have also shown the present and proposed LHC exclusion sensitivities by the dashed red and green contours respectively as taken from [49].

decay to DM (χ or ξ_1) along with jets in final states via hh , hZ , ZZ , W^+W^- modes. The presence of feeble interaction between heavy doublet and the DM ($Y\bar{\Psi}\tilde{H}\chi$) which is the one of requirements of freeze-in scenario makes the heavy neutral state ξ_2 longlived ($c\tau_{\xi_2} > 1$ mm) at the typical scale of detector length. The heavy charged state, ψ^\pm promptly decays to a heavier neutral state, ξ_2 with a soft pion which is difficult to probe. The charge fermion, ψ^\pm can also decay directly into DM with W ($\psi^\pm \rightarrow W^\pm\chi$), which is suppressed when the singlet doublet mixing is small. In the limit of small singlet doublet mixing, the direct and associate productions of $\xi_2 \xi_2$ are one of the promising modes for our analysis which can give rise to displaced vertices with jets plus missing energy signature (DV+MET) before reaching the end of the tracker. Similar kind of search has been performed by ATLAS with $\sqrt{s} = 13$ TeV and $\mathcal{L} = 32.8 \text{ fb}^{-1}$ in the context of split supersymmetric models (i.e. gluino-neutralino) [65]. The displaced events will be analysed by looking at the individual jet tracks which are originating from a displaced vertex. The ATLAS DV+ E_T search estimates the final events targeting at least one displaced vertex with jets and large missing transverse energy. So the signal processes which can give rise to the DV+ E_T signature at LHC in this framework are given as:

$$\begin{aligned}
pp &\rightarrow (\psi^+\psi^-) \rightarrow \bar{\xi}_2 \xi_2 + \text{soft pions} \rightarrow hh/hZ/ZZ + \bar{\chi}\chi \rightarrow \text{jets} + \bar{\chi}\chi; \\
&\rightarrow (\psi^\pm\xi_2) \rightarrow \bar{\xi}_2 \xi_2 + \text{soft pion} \rightarrow hh/hZ/ZZ + \bar{\chi}\chi \rightarrow \text{jets} + \bar{\chi}\chi; \\
&\rightarrow \bar{\xi}_2 \xi_2 \rightarrow hh/hZ/ZZ + \bar{\chi}\chi \rightarrow \text{jets} + \bar{\chi}\chi.
\end{aligned} \tag{4.1}$$

Note that here we have only considered hadronic decay channels of h and Z , since large hadronic branching yields a sizeable cross-section of the $pp \rightarrow \text{jets} + \bar{\chi}\chi$. The above signal cross-section mainly depends on the LLP (long-lived particle) mass, $m_{\xi_2} (\simeq m_\Psi)$ and the

Yukawa coupling, Y . The heavy neutral state, ξ_2 can decay inside (1 mm – 100 m) or outside the detector that crucially depends on the strength of Y .

An accurate prediction of discovery prospects of our proposed scenario requires proper recasting with the exact limits from CMS and ATLAS. One has to perform a careful reconstruction and selection of events employing suitable cuts, and by taking into account the generator-level efficiency along with background estimation. The details of the recasting strategy of this singlet doublet model have been performed in ref.[49]. In Figure 8 we extract the present and proposed exclusion bounds obtained on $m_{\xi_2} - Y$ plane from [49] and check the sensitivities of the benchmark points we used so far, implying different kinds of dark matter dynamics both in standard and non-standard cosmology. The benchmark points FKD-I and FKD-II, which signify pure freeze-in in non-standard cosmology, are inside the 300 fb^{-1} exclusion limit and can be traced in the future runs of ATLAS. One of two benchmark points (KD-II) is also likely to be probed in the next run of ATLAS. If tested, these would probably indicate the presence of modified cosmology with the values of non-standard cosmological parameters as listed in Table 2 and Table 3. The benchmark points labelled as RD-I and RD-II are far outside the reach of ATLAS 300 fb^{-1} run. For these reference points, the decay lengths of ξ_2 turns out to be very large with $c\tau_{\xi_2} \sim \mathcal{O}(1) \text{ km}$. Thus it is challenging to search ξ_2 with such long lifetimes at ATLAS and CMS with current and future sensitivities. The proposed MATHUSLA surface detector experiment [66, 67] could be capable of probing such a long-lived particle. We do not discuss this in detail and refer the readers to [50].

5 Dark matter self-interaction

The present set-up resembles a two-component dark matter framework. We have seen in sections 3.2.1 and 3.2.2, that χ could be the main component with almost 100% relic share owing to the presence of modified cosmology. Hence χ , being adequately abundant in the present Universe, can be an ideal candidate for self-interacting dark matter. As earlier mentioned, few long-standing tensions between astrophysical observations and N-body stimulations for cold DM suggests the DM to be self-interacting with $1 \text{ cm}^2/\text{gm} \lesssim \sigma/m_\chi \lesssim 10 \text{ cm}^2/\text{gm}$ for DM relative velocity ($30 \lesssim v_d \lesssim 200$) km/s [68]. In the present framework, the self interaction can take place through ϕ mediation. We assume the χ to be symmetric in nature. The DM self-interaction processes are $\chi\chi \rightarrow \chi\chi$, $\bar{\chi}\bar{\chi} \rightarrow \bar{\chi}\bar{\chi}$ and $\bar{\chi}\chi \rightarrow \bar{\chi}\chi$. The nonrelativistic self-scattering in DM halos is conventionally described by a Yukawa potential,

$$V(r) = \pm \frac{\alpha_D^2}{4\pi r} e^{-m_\phi r}, \quad (5.1)$$

where “ \pm ” stands for repulsive and attractive potentials. The parameter α_D is the analog of fine structure constant defined by $\alpha_D = \frac{\lambda^2}{4\pi}$. In general, a fermion dark matter can self-interacts via both scalar and vector portal. Note that the scalar interactions are purely attractive, while a vector interaction could be both attractive or repulsive [68]. In literature, uses of two kind of cross sections can be noticed namely (i) transfer cross section (σ_T) and (ii) viscosity cross section (σ_V), which are defined as follows [4, 68–72]:

$$\sigma_T = \int d\Omega (1 - \cos\theta) \frac{d\sigma}{d\Omega}, \quad \sigma_V = \int d\Omega \sin^2\theta \frac{d\sigma}{d\Omega}, \quad (5.2)$$

where θ is the scattering angle. The viscosity cross section has certain merits over the transfer one. For example, the σ_V takes care of the divergences in both forward and backward

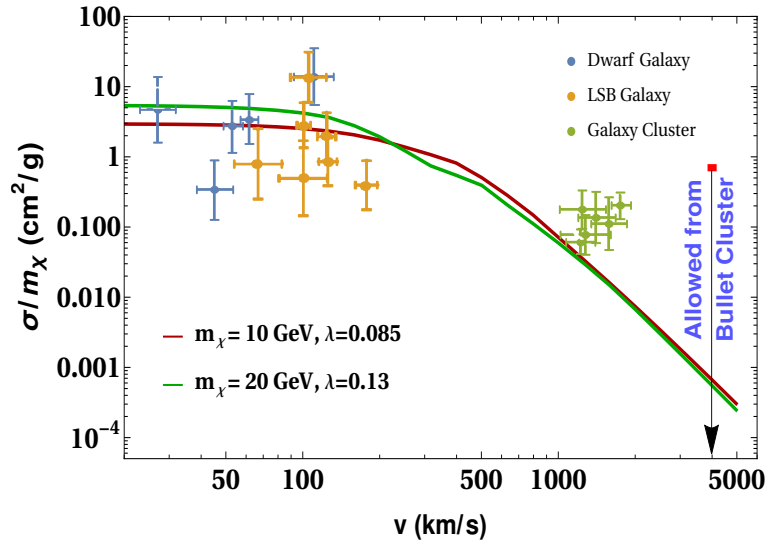


Figure 9. Self-interaction cross section as function of velocity for the two different sets of (m_χ, λ) that have been used to describe the dark matter phenomenology in sections 3.2.1 and 3.2.2. The black arrow indicates the constraint from the Bullet Cluster which is $\frac{\sigma}{m_\chi} < 0.7 \text{ cm}^2/\text{g}$ for $v = 4000 \text{ km/s}$ [4, 13]. We fix m_ϕ at 10 MeV. We also show the observational data from dwarfs (blue), low surface brightness (LSB) galaxies (orange), and clusters (green) as taken from [74].

scatterings in the DM halo. In addition, for self-interaction between identical particles, transfer cross section fails. In view of this, we calculate the σ_V in the present set up.

The description of the self-scattering could be of different natures (classical, semi-classical or quantum), parameterized by two dimensionless parameters $\kappa = \frac{m_\chi v_d}{m_\phi}$ and $\beta = \frac{2\alpha_\chi m_\phi}{m_\chi v_d^2}$ correlated to the momentum and strength of the potential relative to the kinetic energy. The system is known to be in the classical, semi-classical, and quantum regime for $\kappa \gg 1$, $\kappa \gtrsim 1$ and $\kappa \lesssim 1$ respectively. The analytical form of σ_V in classical and semi-classical regimes can be found in ref. [73].

For the quantum case (excluding the Born approximation for $2\beta\kappa^2 \ll 1$), in principle one needs to solve the Schrodinger equation by partial wave analysis in order to compute the differential cross section. The differential scattering cross section can be computed by,

$$\frac{d\sigma}{d\Omega} = \frac{1}{k^2} \left| (2l+1)e^{i\delta_l} P_l(\cos\theta) \sin\delta_l \right|^2. \quad (5.3)$$

where the phase shift for the partial wave is indicated by δ_l . The Schrodinger equation for the radial wave function $R_l(r)$ of the reduced DM two-particle system is written as,

$$\frac{1}{r^2} \frac{\partial}{\partial r} \left(r^2 \frac{dR_l}{dr} \right) + \left(k^2 - \frac{l(l+1)}{r^2} - 2\mu V(r) \right) R_l = 0, \quad (5.4)$$

where $\mu = m_\chi/2$ is the reduced mass and $k = \mu v_d$. Then by obtaining δ_l from the asymptotic form of the radial function $R_l(r)$, one can reach at the approximated expression for the viscosity cross section:

$$\sigma_V m_\phi^2 \simeq \frac{4\pi}{\kappa^2} \int_0^\infty dl \frac{(l + \frac{1}{2})(l + \frac{3}{2})}{2l+2} \sin^2 2\delta'_l \left(l + \frac{1}{2} \right), \quad (5.5)$$

where $\delta'(l + 1/2) \simeq \delta_{l+1} - \delta_l$. The analytical computation of σ_V looks unlikely in the above case, where both quantum and non-resonant effects are important. However, for $\kappa \ll 1$, the S-wave scattering dominates, and the Hulthen potential can be implemented to find the σ_V analytically as indicated in [73].

In Figure 9, we estimate the velocity dependence of the viscosity cross section σ_V considering two sets of (m_χ, λ) as used for the DM analysis earlier in section 3.2.1 and section 3.2.2 with $m_\phi = 10$ MeV. Note that for both the benchmark points, we could obtain nearly same percent relic abundance for the dark matter candidate χ in considering non-standard cosmology namely kination domination or faster than kination domination. For both the (m_χ, λ) sets, the parameter $\frac{\sigma_v}{m_\chi}$ remains in the range (1-10) cm^2/g at $v = (30 - 200)$ km/s. We also found that these points also satisfy the bound $\frac{\sigma_v}{m_\chi} < 0.7 \text{ cm}^2/\text{g}$ at $v = 4000$ km/s, arising from the observations in Bullet Cluster galaxies. In the case of RD dominated Universe, for the two benchmark points under our discussion, χ is not adequately abundant in the present scenario, and hence the solution of small structure anomalies remains unlikely. However, the assumption of a modified cosmology before BBN turns instrumental in the simultaneous realisation of adequately abundant χ component dark matter and sufficient self-interaction to alleviate the small scale anomalies of the Universe.

6 Summary and Conclusion

The singlet doublet model is a simple particle extension of SM, providing a viable dark matter candidate from mixing of doublet and singlet fermions after the electroweak symmetry breaking. Different variants of this scenario are extensively studied for its enriched dark sector and collider signatures. In this work, we have examined whether a non-thermally produced and adequately abundant GeV scale fermion doublet dark matter candidate has the potential to be probed at colliders. We also discuss the prospect of alleviating the small scale structure anomalies of the Universe.

We have minimally extended the singlet doublet dark matter model with a MeV scale singlet scalar, which mediates the dark matter self-interaction. The singlet scalar is stable in Universe lifetime since it has no decay mode. The fermion dark matter has a non-thermal origin and can be produced adequately in the early phase of the Universe. A strong self-interaction, in general, prefers a sizable non-gravitational interaction strength between the dark matter and the mediator particle. With such a notion, our computation indicates the formation of internal dark thermal equilibrium when the conversion process from the fermion dark matter to scalar mediator turns so efficient that it significantly suppresses relic abundance for our dark matter candidate. In fact, the mediator particle emerges to be way more abundant in the present Universe. The process as mentioned above is prominent in a standard radiation-dominated Universe, and we remain unsuccessful in obtaining the singlet doublet fermion dark matter as the main component.

We adopt two specific non-standard cosmological scenarios such as kination and faster than kination-dominated early Universe to circumvent this issue. The motivation for such choices is to suppress the conversion process inside the dark sector. We have found that proper tunings of non-standard cosmological parameters completely alter the evolution patterns of the number densities for the dark sector particles. In fact, the benchmark points which had earlier manifested a reannihilating pattern in the RD dominated Universe depict a pure freeze-in scenario in the non-standard Universe with negligible mediator abundance in the present Universe. In addition, for some choices of the non-standard cosmological parameters,

the dark sector still goes through internal thermal equilibrium. However, that does not cause colossal depletion to the dark matter relic, unlike the case considering radiation domination.

In short, the presence of a modified cosmology helps realise the fermion-dark matter as the main component that is adequately abundant in the present Universe. An exciting consequence comes in terms of collider constraints, where we found that the displaced Vertex signature can provide the robust exclusion bound on the GeV scale DM parameter space. Some of our benchmark points are already within the projected exclusion limit that can be tested by LHC in the next run. We have further demonstrated that the realised parameter space can indeed generate velocity-dependent sufficient self-interactions (consistent with the bounds from observations at bullet cluster galaxies) with a MeV scale mediator.

We conclude with the comment that, in general, a freeze-in dark matter being feebly coupled to the visible sector is extremely hard to track at experiments. Interestingly, the proposed framework of singlet doublet freeze-in GeV scale DM has ample scopes to be indirectly probed *e.g.* in the astrophysical experiments at galaxy scales due to the strong self-interaction of the fermion dark matter as well as in the collider experiments by virtue of modified cosmological theory.

A Cross section

The analytical expression for the cross section of $\chi\chi \rightarrow \phi\phi$ process is given by,

$$\sigma_{\chi\chi \rightarrow \phi\phi} = \frac{1}{32\pi s(s-4m_\chi^2)} \times \left\{ \frac{\ln B}{s-2m_\phi^2} \left[\lambda^4 s^2 - 4\lambda^4 (m_\phi^2 - 4m_\chi^2) s + 6\lambda^4 m_\phi^4 - 16\lambda^4 m_\phi^2 m_\chi^2 - 32\lambda^4 m_\chi^2 \right] - \frac{\sqrt{(s-4m_\chi^2)(s-4m_\phi^2)}}{m_\chi^2 s - 4m_\phi^2 m_\chi^2 + m_\phi^4} \left[\lambda^4 (2m_\chi^2(s+8m_\chi^2) - 16m_\phi^2 m_\chi^2 + 3m_\phi^4) \right] \right\}, \quad (\text{A.1})$$

where

$$B \equiv \frac{s - 2m_\phi^2 + \sqrt{(s-4m_\chi^2)(s-4m_\phi^2)}}{s - 2m_\phi^2 - \sqrt{(s-4m_\chi^2)(s-4m_\phi^2)}}. \quad (\text{A.2})$$

B Decay widths

Before EW symmetry breaking the production of dark matter occurs from $\Psi \rightarrow H\chi$ decay while in the post EW symmetry breaking era, decays such as $\xi_2 \rightarrow h\chi$, $\xi_2 \rightarrow Z\chi$ and $\psi^\pm \rightarrow W^\pm\chi$ turn active. The analytical expression for the decay widths are read as,

$$\Gamma_{\xi_2 \rightarrow h\chi} = \frac{Y^2}{32\pi m_{\xi_2}^3} \{ (m_{\xi_2} + m_\chi)^2 - m_h^2 \} F(m_{\xi_2}, m_\chi, m_h), \quad (\text{B.1})$$

$$\Gamma(\xi_2 \rightarrow Z\chi) = \frac{Y^2}{32\pi} \frac{\{ (m_{\xi_2} - m_\chi)^2 - m_Z^2 \} \{ (m_{\xi_2} - m_\chi)^2 + 2m_Z^2 \}}{m_{\xi_2}^3 (m_{\xi_2} - m_\chi)^2} F(m_{\xi_2}, m_\chi, m_Z), \quad (\text{B.2})$$

$$\Gamma(\psi^\pm \rightarrow W^\pm\chi) = \frac{Y^2}{32\pi} \frac{\{ (m_\Psi - m_\chi)^2 - m_W^2 \} \{ (m_\Psi + m_\chi)^2 + 2m_W^2 \}}{m_\Psi^3 (m_\Psi - m_\chi)^2} F(m_\Psi, m_\chi, m_W), \quad (\text{B.3})$$

where $F(x, y, z) = \sqrt{x^4 + y^4 + z^4 - 2x^2y^2 - 2x^2z^2 - 2y^2z^2}$. We also note that

$$\Gamma_{\Psi \rightarrow H\chi} \simeq 4 \Gamma(\xi_2 \rightarrow h\chi). \quad (\text{B.4})$$

C Energy Transfer rate from SM to dark sector

The aim of this appendix is to determine an analytical form of the energy transfer rate for two body decay of Ψ_i appearing in R.H.S of Eq.(3.4). We start with the Boltzmann equation for the phase-space distribution of a particle species Ψ_i :

$$\frac{\partial f_{\Psi_i}(p_{\Psi_i}, t)}{\partial t} = H(t)p_{\Psi_i} \frac{\partial f_{\Psi_i}(p_{\Psi_i}, t)}{\partial p_{\Psi_i}} + C[f], \quad (\text{C.1})$$

where $C[f]$ is the collision operator for tree level Ψ_i decay. For a specific process $\Psi_i \rightarrow a + b$ process, the collision term takes the following form,

$$C[f] = -\frac{1}{2E_{\Psi_i}} \int d\Pi_a d\Pi_b (2\pi)^4 \delta^{(4)}(p_{\Psi_i} - p_a - p_b) \times \left[|\mathcal{M}_{\Psi_i \rightarrow a+b}|^2 f_{\Psi_i} (1 \pm f_a)(1 \pm f_b) - |\mathcal{M}_{a+b \rightarrow \Psi}|^2 f_a f_b (1 \pm f_{\Psi_i}) \right], \quad (\text{C.2})$$

where $d\Pi_i = \frac{d^3 p_i}{(2\pi)^3 2E_i}$, and “ \pm ” symbolises the Bose-enhancement and Pauli-blocking factors. We have used the Maxwell-Boltzmann distribution approximation and use $f_i \approx e^{-E_i/T_i}$ and $1 \pm f_i \approx 1$ to simplify the calculation. The energy-transfer rate from the SM sector to the dark sector is obtained by

$$\frac{d\rho_{\Psi_i}}{dt} = -3H(P_{\Psi_i} + \rho_{\Psi_i}) + \int \frac{d^3 p_{\Psi_i}}{(2\pi)^3} E_{\Psi_i} C[f]. \quad (\text{C.3})$$

In case for a decay, we write

$$\int \frac{d^3 p_{\Psi_i}}{(2\pi)^3} E_{\Psi_i} C[f] = n_{\Psi_i} \mathcal{P}_{\Psi_i}, \quad (\text{C.4})$$

where we obtain $n_{\Psi_i} \mathcal{P}_{\Psi_i} = n_{\Psi_i} m_{\Psi_i} \Gamma_{\Psi_i}$.

Acknowledgments

PK and SS gratefully acknowledge the HPC resources (Vikram-100 HPC) and TDP project at PRL for the computations. AKS appreciates Sougata Ganguly for several discussions during the course of work. AKS is supported by NPDF grant PDF/2020/000797 from Science and Engineering Research Board, Government of India. PG would like to acknowledge the support from DAE, India for the Regional Centre for Accelerator based Particle Physics (RECAPP), Harish Chandra Research Institute.

Note added:

Shortly before submitting this manuscript, the preprint [75] appeared on the arXiv, which also considers the self-interacting dark matter in an enlarged variant of the singlet doublet framework. The dark sector is purely thermal in their case under the assumption of a standard radiation dominated Universe. In contrast, we have explored a freeze-in production of a hidden dark sector considering a few different variants of cosmological scenarios.

References

- [1] L. J. Hall, K. Jedamzik, J. March-Russell and S. M. West, *Freeze-In Production of FIMP Dark Matter*, *JHEP* **03** (2010) 080 [[0911.1120](#)].
- [2] J. Dubinski and R. G. Carlberg, *The Structure of Cold Dark Matter Halos*, *Astrophysical Journal* **378** (1991) 496.
- [3] R. A. Flores and J. R. Primack, *Observational and theoretical constraints on singular dark matter halos*, *Astrophys. J. Lett.* **427** (1994) L1 [[astro-ph/9402004](#)].
- [4] S. Tulin, H.-B. Yu and K. M. Zurek, *Beyond Collisionless Dark Matter: Particle Physics Dynamics for Dark Matter Halo Structure*, *Phys. Rev. D* **87** (2013) 115007 [[1302.3898](#)].
- [5] M. Boylan-Kolchin, J. S. Bullock and M. Kaplinghat, *Too big to fail? the puzzling darkness of massive milky way subhaloes*, *Monthly Notices of the Royal Astronomical Society: Letters* **415** (2011) L40–L44.
- [6] M. A. Zwaan, M. J. Meyer and L. Staveley-Smith, *The velocity function of gas-rich galaxies*, *Monthly Notices of the Royal Astronomical Society* **403** (2010) 1969–1977.
- [7] D. N. Spergel and P. J. Steinhardt, *Observational evidence for selfinteracting cold dark matter*, *Phys. Rev. Lett.* **84** (2000) 3760 [[astro-ph/9909386](#)].
- [8] J. S. Bullock and M. Boylan-Kolchin, *Small-Scale Challenges to the Λ CDM Paradigm*, *Ann. Rev. Astron. Astrophys.* **55** (2017) 343 [[1707.04256](#)].
- [9] A. A. Klypin, A. V. Kravtsov, O. Valenzuela and F. Prada, *Where are the missing Galactic satellites?*, *Astrophys. J.* **522** (1999) 82 [[astro-ph/9901240](#)].
- [10] B. Moore, S. Ghigna, F. Governato, G. Lake, T. R. Quinn, J. Stadel et al., *Dark matter substructure within galactic halos*, *Astrophys. J. Lett.* **524** (1999) L19 [[astro-ph/9907411](#)].
- [11] B. Moore, T. R. Quinn, F. Governato, J. Stadel and G. Lake, *Cold collapse and the core catastrophe*, *Mon. Not. Roy. Astron. Soc.* **310** (1999) 1147 [[astro-ph/9903164](#)].
- [12] V. Springel, J. Wang, M. Vogelsberger, A. Ludlow, A. Jenkins, A. Helmi et al., *The Aquarius Project: the subhalos of galactic halos*, *Mon. Not. Roy. Astron. Soc.* **391** (2008) 1685 [[0809.0898](#)].
- [13] S. W. Randall, M. Markevitch, D. Clowe, A. H. Gonzalez and M. Bradac, *Constraints on the Self-Interaction Cross-Section of Dark Matter from Numerical Simulations of the Merging Galaxy Cluster 1E 0657-56*, *Astrophys. J.* **679** (2008) 1173 [[0704.0261](#)].
- [14] C. Kouvaris, I. M. Shoemaker and K. Tuominen, *Self-Interacting Dark Matter through the Higgs Portal*, *Phys. Rev. D* **91** (2015) 043519 [[1411.3730](#)].
- [15] K. Kainulainen, K. Tuominen and V. Vaskonen, *Self-interacting dark matter and cosmology of a light scalar mediator*, *Phys. Rev. D* **93** (2016) 015016 [[1507.04931](#)].
- [16] D. Borah, M. Dutta, S. Mahapatra and N. Sahu, *Muon ($g - 2$) and XENON1T excess with boosted dark matter in $L\mu - L\tau$ model*, *Phys. Lett. B* **820** (2021) 136577 [[2104.05656](#)].
- [17] M. Dutta, S. Mahapatra, D. Borah and N. Sahu, *Self-interacting Inelastic Dark Matter in the light of XENON1T excess*, *Phys. Rev. D* **103** (2021) 095018 [[2101.06472](#)].
- [18] D. Borah, M. Dutta, S. Mahapatra and N. Sahu, *Boosted Self-Interacting Dark Matter and XENON1T Excess*, [2107.13176](#).
- [19] M. Duch, B. Grzadkowski and D. Huang, *Strongly self-interacting vector dark matter via freeze-in*, *JHEP* **01** (2018) 020 [[1710.00320](#)].
- [20] Y. Du, F. Huang, H.-L. Li and J.-H. Yu, *Freeze-in Dark Matter from Secret Neutrino Interactions*, *JHEP* **12** (2020) 207 [[2005.01717](#)].

- [21] F. D’Eramo, *Dark matter and Higgs boson physics*, *Phys. Rev. D* **76** (2007) 083522 [[0705.4493](#)].
- [22] R. Enberg, P. J. Fox, L. J. Hall, A. Y. Papaioannou and M. Papucci, *LHC and dark matter signals of improved naturalness*, *JHEP* **11** (2007) 014 [[0706.0918](#)].
- [23] T. Cohen, J. Kearney, A. Pierce and D. Tucker-Smith, *Singlet-Doublet Dark Matter*, *Phys. Rev. D* **85** (2012) 075003 [[1109.2604](#)].
- [24] C. Cheung and D. Sanford, *Simplified Models of Mixed Dark Matter*, *JCAP* **02** (2014) 011 [[1311.5896](#)].
- [25] D. Restrepo, A. Rivera, M. Sánchez-Peláez, O. Zapata and W. Tangarife, *Radiative Neutrino Masses in the Singlet-Doublet Fermion Dark Matter Model with Scalar Singlets*, *Phys. Rev. D* **92** (2015) 013005 [[1504.07892](#)].
- [26] L. Calibbi, A. Mariotti and P. Tziveloglou, *Singlet-Doublet Model: Dark matter searches and LHC constraints*, *JHEP* **10** (2015) 116 [[1505.03867](#)].
- [27] S. Bhattacharya, N. Sahoo and N. Sahu, *Minimal vectorlike leptonic dark matter and signatures at the LHC*, *Phys. Rev. D* **93** (2016) 115040 [[1510.02760](#)].
- [28] C. E. Yaguna, *Singlet-Doublet Dirac Dark Matter*, *Phys. Rev. D* **92** (2015) 115002 [[1510.06151](#)].
- [29] S. Horiuchi, O. Macias, D. Restrepo, A. Rivera, O. Zapata and H. Silverwood, *The Fermi-LAT gamma-ray excess at the Galactic Center in the singlet-doublet fermion dark matter model*, *JCAP* **03** (2016) 048 [[1602.04788](#)].
- [30] S. Banerjee, S. Matsumoto, K. Mukaida and Y.-L. S. Tsai, *WIMP Dark Matter in a Well-Tempered Regime: A case study on Singlet-Doublets Fermionic WIMP*, *JHEP* **11** (2016) 070 [[1603.07387](#)].
- [31] T. Abe, *Effect of CP violation in the singlet-doublet dark matter model*, *Phys. Lett. B* **771** (2017) 125 [[1702.07236](#)].
- [32] N. Maru, N. Okada and S. Okada, *Fermionic Minimal Dark Matter in 5D Gauge-Higgs Unification*, *Phys. Rev. D* **96** (2017) 115023 [[1801.00686](#)].
- [33] N. Maru, T. Miyaji, N. Okada and S. Okada, *Fermion Dark Matter in Gauge-Higgs Unification*, *JHEP* **07** (2017) 048 [[1704.04621](#)].
- [34] S. Bhattacharya, N. Sahoo and N. Sahu, *Singlet-Doublet Fermionic Dark Matter, Neutrino Mass and Collider Signatures*, *Phys. Rev. D* **96** (2017) 035010 [[1704.03417](#)].
- [35] Q.-F. Xiang, X.-J. Bi, P.-F. Yin and Z.-H. Yu, *Exploring Fermionic Dark Matter via Higgs Boson Precision Measurements at the Circular Electron Positron Collider*, *Phys. Rev. D* **97** (2018) 055004 [[1707.03094](#)].
- [36] S. Esch, M. Klasen and C. E. Yaguna, *A singlet doublet dark matter model with radiative neutrino masses*, *JHEP* **10** (2018) 055 [[1804.03384](#)].
- [37] G. Arcadi, *2HDM portal for Singlet-Doublet Dark Matter*, *Eur. Phys. J. C* **78** (2018) 864 [[1804.04930](#)].
- [38] A. Dutta Banik, A. K. Saha and A. Sil, *Scalar assisted singlet doublet fermion dark matter model and electroweak vacuum stability*, *Phys. Rev. D* **98** (2018) 075013 [[1806.08080](#)].
- [39] S. Bhattacharya, P. Ghosh, N. Sahoo and N. Sahu, *Mini Review on Vector-Like Leptonic Dark Matter, Neutrino Mass, and Collider Signatures*, *Front. in Phys.* **7** (2019) 80 [[1812.06505](#)].
- [40] J. Fiaschi, M. Klasen and S. May, *Singlet-doublet fermion and triplet scalar dark matter with radiative neutrino masses*, *JHEP* **05** (2019) 015 [[1812.11133](#)].

- [41] B. Barman, S. Bhattacharya, P. Ghosh, S. Kadam and N. Sahu, *Fermion Dark Matter with Scalar Triplet at Direct and Collider Searches*, *Phys. Rev. D* **100** (2019) 015027 [[1902.01217](#)].
- [42] D. Restrepo, A. Rivera and W. Tangarife, *Singlet-Doublet Dirac Dark Matter and Neutrino Masses*, *Phys. Rev. D* **100** (2019) 035029 [[1906.09685](#)].
- [43] B. Barman, D. Borah, P. Ghosh and A. K. Saha, *Flavoured gauge extension of singlet-doublet fermionic dark matter: neutrino mass, high scale validity and collider signatures*, *JHEP* **10** (2019) 275 [[1907.10071](#)].
- [44] P. Konar, A. Mukherjee, A. K. Saha and S. Show, *Linking pseudo-Dirac dark matter to radiative neutrino masses in a singlet-doublet scenario*, *Phys. Rev. D* **102** (2020) 015024 [[2001.11325](#)].
- [45] P. Konar, A. Mukherjee, A. K. Saha and S. Show, *A dark clue to seesaw and leptogenesis in a pseudo-Dirac singlet doublet scenario with (non)standard cosmology*, *JHEP* **03** (2021) 044 [[2007.15608](#)].
- [46] M. Dutta, S. Bhattacharya, P. Ghosh and N. Sahu, *Singlet-Doublet Majorana Dark Matter and Neutrino Mass in a minimal Type-I Seesaw Scenario*, *JCAP* **03** (2021) 008 [[2009.00885](#)].
- [47] B. Barman, P. Ghosh, F. S. Queiroz and A. K. Saha, *Scalar multiplet dark matter in a fast expanding Universe: Resurrection of the desert region*, *Phys. Rev. D* **104** (2021) 015040 [[2101.10175](#)].
- [48] D. Borah, M. Dutta, S. Mahapatra and N. Sahu, *Lepton Anomalous Magnetic Moment with Singlet-Doublet Fermion Dark Matter in Scotogenic $U(1)_{L_\mu-L_\tau}$ Model*, [2109.02699](#).
- [49] L. Calibbi, L. Lopez-Honorez, S. Lowette and A. Mariotti, *Singlet-Doublet Dark Matter Freeze-in: LHC displaced signatures versus cosmology*, *JHEP* **09** (2018) 037 [[1805.04423](#)].
- [50] J. M. No, P. Tunney and B. Zaldivar, *Probing Dark Matter freeze-in with long-lived particle signatures: MATHUSLA, HL-LHC and FCC-hh*, *JHEP* **03** (2020) 022 [[1908.11387](#)].
- [51] B. Zhu and M. Abdughani, *Thermal Relic of Self-Interacting Dark Matter with Retarded Decay of Mediator*, [2103.06050](#).
- [52] G. Krnjaic, *Freezing In, Heating Up, and Freezing Out: Predictive Nonthermal Dark Matter and Low-Mass Direct Detection*, *JHEP* **10** (2018) 136 [[1711.11038](#)].
- [53] J. Berger, D. Croon, S. El Hedri, K. Jedamzik, A. Perko and D. G. E. Walker, *Dark matter amnesia in out-of-equilibrium scenarios*, *JCAP* **02** (2019) 051 [[1812.08795](#)].
- [54] C. Cheung, G. Elor, L. J. Hall and P. Kumar, *Origins of Hidden Sector Dark Matter I: Cosmology*, *JHEP* **03** (2011) 042 [[1010.0022](#)].
- [55] C. Cheung, G. Elor, L. J. Hall and P. Kumar, *Origins of Hidden Sector Dark Matter II: Collider Physics*, *JHEP* **03** (2011) 085 [[1010.0024](#)].
- [56] X. Chu, T. Hambye and M. H. G. Tytgat, *The Four Basic Ways of Creating Dark Matter Through a Portal*, *JCAP* **05** (2012) 034 [[1112.0493](#)].
- [57] F. D’Eramo, N. Fernandez and S. Profumo, *When the Universe Expands Too Fast: Relentless Dark Matter*, *JCAP* **05** (2017) 012 [[1703.04793](#)].
- [58] PLANCK collaboration, *Planck 2018 results. VI. Cosmological parameters*, *Astron. Astrophys.* **641** (2020) A6 [[1807.06209](#)].
- [59] A. Hryczuk and M. Laletin, *Dark matter freeze-in from semi-production*, *JHEP* **06** (2021) 026 [[2104.05684](#)].
- [60] A. Tapadar, S. Ganguly and S. Roy, *Non-adiabatic evolution of dark sector in the presence of $U(1)_{L_\mu-L_\tau}$ gauge symmetry*, [2109.13609](#).

- [61] P. Konar, R. Roshan and S. Show, *Freeze-in Dark Matter Through Forbidden Channel in $U(1)_{B-L}$* , [2110.14411](#).
- [62] S. Bhattacharya, P. Ghosh and N. Sahu, *Multipartite dark matter with scalars, fermions and signatures at lhc*, *Journal of High Energy Physics* **2019** (2019) .
- [63] ATLAS collaboration, *Search for long-lived charginos based on a disappearing-track signature in pp collisions at $\sqrt{s} = 13$ TeV with the ATLAS detector*, *JHEP* **06** (2018) 022 [[1712.02118](#)].
- [64] CMS collaboration, *Search for disappearing tracks as a signature of new long-lived particles in proton-proton collisions at $\sqrt{s} = 13$ TeV*, *JHEP* **08** (2018) 016 [[1804.07321](#)].
- [65] ATLAS collaboration, *Search for long-lived, massive particles in events with displaced vertices and missing transverse momentum in $\sqrt{s} = 13$ TeV pp collisions with the ATLAS detector*, *Phys. Rev. D* **97** (2018) 052012 [[1710.04901](#)].
- [66] D. Curtin et al., *Long-Lived Particles at the Energy Frontier: The MATHUSLA Physics Case*, *Rept. Prog. Phys.* **82** (2019) 116201 [[1806.07396](#)].
- [67] MATHUSLA collaboration, *A Letter of Intent for MATHUSLA: A Dedicated Displaced Vertex Detector above ATLAS or CMS.*, [1811.00927](#).
- [68] S. Tulin and H.-B. Yu, *Dark Matter Self-interactions and Small Scale Structure*, *Phys. Rept.* **730** (2018) 1 [[1705.02358](#)].
- [69] M. R. Buckley and P. J. Fox, *Dark Matter Self-Interactions and Light Force Carriers*, *Phys. Rev. D* **81** (2010) 083522 [[0911.3898](#)].
- [70] J. L. Feng, M. Kaplinghat and H.-B. Yu, *Halo Shape and Relic Density Exclusions of Sommerfeld-Enhanced Dark Matter Explanations of Cosmic Ray Excesses*, *Phys. Rev. Lett.* **104** (2010) 151301 [[0911.0422](#)].
- [71] R. N. Mohapatra, S. Nussinov and V. L. Teplitz, *Mirror matter as selfinteracting dark matter*, *Phys. Rev. D* **66** (2002) 063002 [[hep-ph/0111381](#)].
- [72] W. G. Vincenti and C. H. Kruger, *Introduction to physical gas dynamics*. 1965.
- [73] B. Colquhoun, S. Heeba, F. Kahlhoefer, L. Sagunski and S. Tulin, *Semiclassical regime for dark matter self-interactions*, *Phys. Rev. D* **103** (2021) 035006 [[2011.04679](#)].
- [74] M. Kaplinghat, S. Tulin and H.-B. Yu, *Dark Matter Halos as Particle Colliders: Unified Solution to Small-Scale Structure Puzzles from Dwarfs to Clusters*, *Phys. Rev. Lett.* **116** (2016) 041302 [[1508.03339](#)].
- [75] D. Borah, M. Dutta, S. Mahapatra and N. Sahu, *Singlet-Doublet Self-interacting Dark Matter and Radiative Neutrino Mass*, [2112.06847](#).